International Journal of
Advanced Thermofluid Research

ISSN 2455-1368
www.ijatr.org

Rotating Fluid Flow on MHD Radiative Nanofluid past a Stretching Sheet

M. Shakhaoath Khan[1], M. Mahmud Alam[1], M. Ferdows[2*], E. E. Tzirtzilakis[3], Ifsana Karim[1] and Shuyu Sun[4]

[1]Mathematics Discipline; Science, Engineering and Technology School, Khulna University, Khulna-9208, Bangladesh.
[2]Research Group of Fluid Flow Modeling and Simulation, Department of Applied Mathematics, University of Dhaka, Dhaka-1000, Bangladesh.
[3]Fluid Dynamics &Turbomachinery Laboratory, Department of Mechanical Engineering, Technological Educational Institute of Western Greece, 1 M. AleksandrouStr, Koukouli, 263 34 Patras Greece.
[4]Division of Applied Mathematics and Computational Science, King Abduallah University of Science and Technology, Thuwal, Saudi Arabia.

Keywords
Nanofluid • Magnetic Field • Radiation • Stretching Sheet • Rotating System.

Received
April 2, 2016
Revised
May 13, 2016
Accepted
May 18, 2016
Published
June 1, 2016

Abstract

The present study is aimed at examining the unsteady MHD heat and mass flow of a nanofluid passing a stretching sheet with thermal radiation in a rotating system. The governing boundary layer equations as continuity, momentum, energy, concentration equation were solved by introducing a time dependent length scale in a similarity approach. Obtained nonlinear coupled equations along with the appropriate boundary conditions are then solved by Nactsheim-Swigert shooting iteration technique together with Runge-Kutta six order scheme. The effect of different dimensionless parameters on the flow field as magnetic parameter, rotational parameter, radiation parameter, Prandtl number, Eckert number, Lewis number, Brownian motion parameter, thermophoresis parameter was investigated. The distribution of the primary velocity, secondary velocity, temperature, concentration, local skin-friction coefficients, Nusselt number and the Sherwood number with the effect of the important parameters entering into the problem separately and reported graphically.

***Corresponding email**: ferdows@du.ac.bd (M. Ferdows).

DOI: https://doi.org/10.51141/IJATR.2016.2.1.2

Nomenclature

a	Empirical constants
B_0	Magnetic induction
C	Nanoparticle concentration
C_w	Nanoparticle concentration at stretching surface

C_∞ Ambient nanoparticle concentration as y tends to infinity
c_p Specific heat capacity, J kg^{-1} K^{-1}
D_B Brownian diffusion coefficient
D_T Thermophoresis diffusion coefficient
K Radiation Parameter
L_e Lewis number
M Magnetic parameter
N_u Nusselt number
N_b Brownian motion parameter
N_t Thermophoresis parameter
P fluid pressure, Pa
P_r Prandtl number
R Rotational parameter
S_h Sherwood number
t Time, s
T Fluid temperature, K
T_w Temperature at the stretching surface, K
T_∞ Ambient temperature as y tends to infinity , K
v Velocity components along y axes, ms^{-1}
u_w Stretching surface velocity, ms^{-1}
x, y Cartesian coordinates measured along stretching surface, m

Greek Symbols
ν Kinematic viscosities, m^2 s^{-1}
$(\rho c)_p$ Effective heat capacity of the nanofluid, J m^{-3}K^{-1}
$(\rho c)_f$ Heat capacity of the fluid, J m^{-3}K^{-1}
α Thermal diffusivity, m^2 s^{-1}
η Similarity variable
ψ Stream function
τ_x, τ_z Skin-friction coefficients
$f(\eta)$ Dimensionless primary velocity
$g(\eta)$ Dimensionless secondary velocity
$\theta(\eta)$ Dimensionless temperature
$\varphi(\eta)$ Dimensionless concentration

1. Introduction

The study of Magnetohydrodynamics (MHD) heat and mass transfer laminar flow by stretching surfaces has generated much interest in recent years. This study finds applications in many engineering disciplines, and industrial manufacturing processes such as aerodynamic extrusion of plastic sheets, polymer extrusion, melt-spinning process, manufacture of plastic and rubber sheets, glass blowing, continuous casting, spinning of fibers, etc. The quality of the resulting sheeting material, as well as the cost of production, may be affected by the speed of collection and the heat transfer rate. Sakiadis (1961) was the pioneer to investigate the boundary-layer behaviour on a continuous solid surface. The thermal radiation effect is a new dimension added to

the study of stretching surface, which has important applications in physics and engineering. The effect of radiation on heat transfer problems has been studied by Hossain and Takhar(1996) and Takhar et al. (1996).

The Coriolis force is very significant as compared to viscous and inertia forces occurring in the basic fluid dynamics. It is generally admitted that the Coriolis force due to Earth's rotation has a strong effect on the hydromagnetic flow in the Earth's liquid core. The study of such fluid flow problem is important due to its applications in various branches of geophysics, astrophysics and fluid engineering. From the point of applications in solar physics and cosmic fluid dynamics, it is important to consider the effects of the electromagnetic and rotation forces on the flow. Considering this aspect of the rotational flows, model studies were carried out on MHD free convection and mass transfer flows in a rotating system by Raptis and Singh (1985) and Singh and Singh (1989). Nazmul and Alam (2008) investigated the effects of Dufor and Soret on unsteady MHD free convection and mass transfer fluid flow through a porous medium in a rotating system.

In recent years nanotechnology has been widely used in many industrial applications. A nanofluid is a term initially used by Choi (1995), which is a colloidal solution of nano-sized solid particles in liquids. The natural convective boundary layer flows of a nanofluid past a vertical plate have described by Kuznestov and Neild (2010). Bachok et al. (2010) has shown the steady boundary layer flow of a nanofluid past a moving semi-infinite flat plate in a uniform free stream. Khan and Pop (2010-11) formulated the problem of laminar boundary layer flow of a nanofluid past a stretching sheet. Khan et al. (2011a&b) investigated the effects of thermal radiation and magnetic field on the boundary layer flow of a nanofluid past a stretching sheet (steady as well as unsteady case for the corresponding problem). Takabi et al. (2014 & 2015) have used the single-phase model for investigation of heat and fluid flow in nanofluids. This model was found accurate enough to capture the thermal and hydrodynamic effects of a nanofluid flow. Very recently a number of boundary layer nanofluid flow studies were reported in the literature (Ferdows et al., 2012 & 2014; Khan et al., 2012, 2013 & 2014; Beg et al., 2014; Wahiduzzamanet al., 2015a&b); however the effect of rotating flow was overlooked.

The present study investigates the rotating effects on MHD boundary layer nanofluid flow over an unsteady stretching surface with the influence of thermal radiation and magnetic field. Similarity the corresponding momentum, energy and concentration equations are derived by introducing a time dependent length scale. These nonlinear coupled equations along with the appropriate boundary conditions are then solved by employing Nactsheim-Swigert(1965) shooting technique together with Runge-Kutta six order iteration schemes.

2. Mathematical Model of the flow

The physical configuration and coordinate system are shown in Figure 1. Considering the Cartesian coordinates, x is measured along the stretching surface and y is normal to the stretching surface.

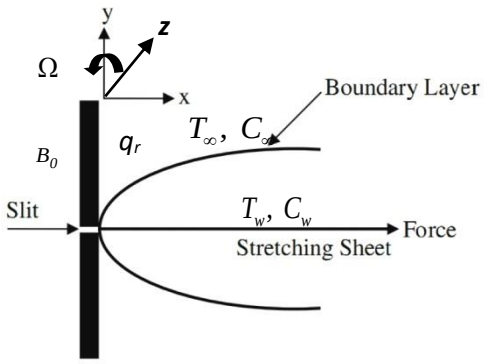

Figure 1.Physical Configuration and coordinates.

Initially the fluid as well as the sheet is at rest, and then the whole system is allowed to rotate with a constant angular velocity Ω about the y -axis. Since the system rotates about $y-\text{axis},\ \mathbf{\Omega}=(0,-\Omega,0)$ is considered. An unsteady uniform stress leading to equal and opposite forces is applied along the x -axis. It is assumed that fluid and the plate before the plate is moved with a constant velocity u_w in its own plane. Instantaneously at time $t>0$, temperature of the plate and species concentration are raised to $T_w\,(>T_\infty)$ and $C_w\,(>C_\infty)$ respectively, which are thereafter maintained constant; T_w, C_w are temperature and species concentrations at the wall while T_∞, C_∞ denote the corresponding values far away from the plate. A uniform magnetic field B_0 is imposed to the plate, where B_0 can be taken as $B=(0,B_0,0)$ and q_r is the radiative heat flux in the y-direction. Under the usual boundary layer approximation, the MHD unsteady nanofluid flow and heat and mass transfer with the radiation effect in a rotating system are governed by the following equations:

The Continuity equation:

$$\frac{\partial v}{\partial y}=0 \tag{1}$$

The Momentum equations:

$$\frac{\partial u}{\partial t}+v\frac{\partial u}{\partial y}-2\Omega w=\upsilon\frac{\partial^2 u}{\partial y^2}-\frac{\sigma' B_0^{\,2}}{\rho}u \tag{2}$$

$$\frac{\partial w}{\partial t}+v\frac{\partial w}{\partial y}+2\Omega w=\upsilon\frac{\partial^2 w}{\partial y^2}-\frac{\sigma' B_0^{\,2}}{\rho}u \tag{3}$$

The Energy equation:

$$\frac{\partial T}{\partial t}+v\frac{\partial T}{\partial y}=\alpha\frac{\partial^2 T}{\partial y^2}-\frac{\alpha}{k}\frac{\partial q_r}{\partial y}+\frac{\upsilon}{c_p}\left(\frac{\partial u}{\partial y}+\frac{\partial w}{\partial y}\right)^2+\tau\left\{D_B\left(\frac{\partial T}{\partial y}\cdot\frac{\partial C}{\partial y}\right)+\frac{D_T}{T_\infty}\left(\frac{\partial T}{\partial y}\right)^2\right\} \tag{4}$$

The Concentration equation:

$$\frac{\partial C}{\partial t}+v\frac{\partial C}{\partial y}=D_B\frac{\partial^2 C}{\partial y^2}+\frac{D_T}{T_\infty}\frac{\partial^2 T}{\partial y^2} \tag{5}$$

The boundary conditions:

$t\le 0;\ u=0,\ w=0, v=0,\ T=T_\infty,\ C=C_\infty$ for all values of y

$t>0;\ u=u_w=ax,\ w=0, v=0,\ T=T_w,\ C=C_w$ at $y=0$

$t>0;\ u=0, w=0\ T\to T_\infty, C\to C_\infty$ as $y\to\infty$ (6)

where, x is the coordinate measured along stretching surface, u_w is the stretching velocity, a is the linear stretching constant, c_p is the specific heat at constant pressure, α is the thermal diffusivity, v is the kinematic viscosity of the fluid, ρ is density of fluid, D_B is the Brownian diffusion coefficient, and D_T is the thermophoresis diffusion coefficient.

Rosseland approximation (Brewster, 1992) has been considered for radiative heat flux and leads to the form as:

$$q_r=-\frac{4\sigma_1}{3\kappa^*}\frac{\partial T^4}{\partial y} \tag{7}$$

where, σ_1 is the Stefan-Boltzmann constant and κ^* is the mean absorption coefficient. In order to obtain similar solutions we introduce a similarity parameter σ as:

$$\sigma=\sigma(t) \tag{8}$$

Such that σ is the time dependent length scale. In terms of this long scale, a convenient solution of equation (1) is considered to be;

$$v=-v_\circ\frac{\nu}{\sigma}. \tag{9}$$

Here $v_\circ$ represents a dimensionless normal velocity at the plate which is positive for suction and negative for blowing. In order to obtain a similarity solution to the equations (1) to (5) with the boundary conditions (6) the following dimensionless variables are used:

$$\eta=\frac{y}{\delta},\ u=U_\circ f, v=-v_\circ\frac{\nu}{\delta},\ w=U_\circ g_\circ, \theta(\eta)=\frac{T-T_\infty}{T_w-T_\infty}, \varphi(\eta)=\frac{C-C_\infty}{C_w-C_\infty} \tag{10}$$

By introducing equations (9) and (10) into equations (2)-(5):

$$-\frac{\sigma}{\nu}\frac{\partial\sigma}{\partial t}\eta f^{/}-v_{\circ}f^{/}=f^{//}-Mf+2Rg_{\circ} \tag{11}$$

$$-\frac{\sigma}{\nu}\frac{\partial\sigma}{\partial t}\eta g_{\circ}^{/}-v_{\circ}g_{\circ}^{/}=g_{\circ}^{//}-2Rf^{/}-Mg_{\circ} \tag{12}$$

$$-\frac{\sigma}{\nu}\frac{\partial\sigma}{\partial t}\eta\theta^{/}-v_{\circ}\theta^{/}=\left(\frac{1+K}{P_r}\right)\theta^{//}+E_c\left(f^{/}+g_{\circ}^{/}\right)^2+N_b\theta^{/}\varphi^{/}+N_t\theta^{/2} \tag{13}$$

$$-\frac{\sigma}{\nu}\frac{\partial\sigma}{\partial t}\eta\varphi^{/}-v_{\circ}\varphi^{/}=\frac{1}{L_e}\left(\varphi^{//}+\frac{N_t}{N_b}\theta^{//}\right), \tag{14}$$

where, the notation primes denote differentiation with respect to η and the parameters are defined by:

Magnetic parameter $M=\frac{\sigma B_0^{\,2}}{\rho a}$, Rotational parameter $R=\frac{\Omega\sigma^2}{\nu}$, Radiation parameter $K=\frac{16\sigma T_\infty^{\,3}}{3k\kappa^*}$, Prandtl number $p_r=\frac{\upsilon}{\alpha}$, Eckert number $E_c=\frac{u_w^{\,2}}{c_p(T_w-T_\infty)}$, Lewis number $L_e=\frac{\upsilon}{D_B}$, Brownian motion parameter $N_b=\frac{(\rho c)_p D_B\left(C_w-C_\infty\right)}{\upsilon(\rho c)_f}$ and Thermophoresis parameter $N_t=\frac{(\rho c)_p D_T\left(T_w-T_\infty\right)}{\upsilon T_\infty(\rho c)_f}$.

The equations (11)-(14) are similar except for the term $\frac{\sigma}{\nu}\frac{\partial\sigma}{\partial t}$ where time t appears explicitly. Thus the similarity conditions require that $\frac{\sigma}{\nu}\frac{\partial\sigma}{\partial t}$ in equations (11)-(14) must be a constant quantity. Hence following the work of Sattar and Alam(1994) one can try a class of solutions of the equations (11)-(14) by assuming that:

$$\frac{\sigma}{\nu}\frac{\partial\sigma}{\partial t}=c\,(\text{a constant}) \tag{15}$$

By integrating Eq. (15):

$$\sigma=\sqrt{2cvt} \tag{16}$$

where the constant of integration is determined through the condition that $\sigma=0$ when $t=0$. It thus appears from (16) that, by making a realistic choice of c to be equal to 2 in Eq. (15) the length

scale σ becomes equal to $\sigma = 2\sqrt{\nu t}$ which exactly corresponds to the usual scaling factor considered for various unsteady boundary layer flows (Schlichting, 1968). Since σ is a scaling factor as well as a similarity parameter, any other value of c in Eq. (15) would not change the nature of solution except that the scale would be different. Finally, by introducing Eq. (15) with $c=2$ in Eqs. (11)-(14), the following dimensionless ordinary differential equations are obtained:

$$f''' + 2\xi f'' - Mf + 2Rg_\circ = 0 \tag{17}$$

$$g_\circ''' + 2\xi g_\circ' - 2Rf - Mg_\circ = 0 \tag{18}$$

$$(1+K)P_r^{-1}\theta''' + 2\xi\theta'' + E_c\left(f'' + g_\circ'\right)^2 + N_b\theta'\varphi' + N_t\theta'^2 = 0 \tag{19}$$

$$\varphi''' + 2L_e\xi\varphi'' + \frac{N_t}{N_b}\theta''' = 0 \tag{20}$$

where, $\xi = \eta + \frac{v_0}{2}$.

The corresponding boundary conditions:

$$\left.\begin{array}{ll} f = 1,\ g_\circ = 0,\ \theta = 1,\ \varphi = 1, & at\ \eta = 0 \\ f = 0,\ g_\circ = 0,\ \theta = 0,\ \varphi = 0, & as\ \eta \to \infty \end{array}\right\} \tag{21}$$

3. Skin-friction coefficients, Nusselt number and Sherwood number

The quantities of chief physical interest are the skin friction coefficient, the Nusselt number (N_u) and the Sherwood number (S_h). The equation defining the components (x, y) of wall skin frictions are $m(u/y)_{y=0}$ and $m(w/y)_{y=0}$, which are proportional to $(f/h)_{h=0}$ and $(g_0/h)_{h=0}$ respectively. N_u is proportional to $(T/y)_{y=0}$, hence we obtain $N_u \quad q(0)$; S_h is proportional to $(C/y)_{y=0}$, so $S_h \quad f(0)$ is obtained. The numerical values of the skin-friction coefficients, N_u and S_h are sorted in Table 1 and Table 2.

4. Numerical Technique

The governing differential equations (17)-(20) are coupled with each other and it is almost impossible to have an analytical solution. Thus computations have been carried out based on numerical technique. The values of the governing parameters are chosen arbitrarily. The system of non-dimensional, nonlinear, coupled ordinary differential equations (17) to (20) with boundary condition (21) were solved numerically by using standard initial value solver (the shooting method). The Nactsheim-Swigert(1965) shooting iteration technique together with Runge-Kutta six order iteration scheme was taken, and the velocity, temperature and concentration were

determined as function of η. There are four asymptotic boundary conditions and hence four unknown surface conditions, $f'(0), g_\circ'(0), \theta'(0)$ and $\varphi'(0)$.

5. Results and Discussion

The velocity profiles for x and z components of velocity, commonly known as non-dimensional primary (f) and secondary velocities $(g_\circ)$, and temperature (q) and concentration (j) profiles are shown in Figures 2-14 for different values of *M, R, K, Pr, Ec, Lc , Nb and Nb* respectively. Figure 2 displays the dimensionless primary velocity distribution $f(\eta)$ for different values of *M* where the other dimensionless parameters are retained as $K = 1.0, R = 0.2, P_r = 0.71, L_e = 10, N_t = 0.1, N_b = 0.1, E_c = 0.01$ *and* $\xi = 0.5$. It can be seen that the primary velocity profiles decrease as *M* increases. With regard to the effect of *R* on velocity distribution, Figure 3 shows that $f(\eta)$ decreases as *R* increases, while the dimensionless secondary velocity distribution $g_\circ(\eta)$ profiles increase as the M increases (Figure 4). Magnetic parameter has a strong impact on the velocity flow field as magnetic field exerts a more dominant role than increasing unsteadiness of the system. The locations of minimum velocities tend to go to lower by increasing the Magnetic parameter this is because the velocity (secondary) is still effectively increased owing to the retarding nature of the magnetic field and the upswing of the momentum boundary layer thickness. With regard to the effects of other parameters, $g_\circ(\eta)$ profiles increase for increasing *R* (Figure 5), decrease with increase of E_c (Figure 6), N_t *and* N_b (Figure 7), and increase gradually with increase of *K* (Figure 8).

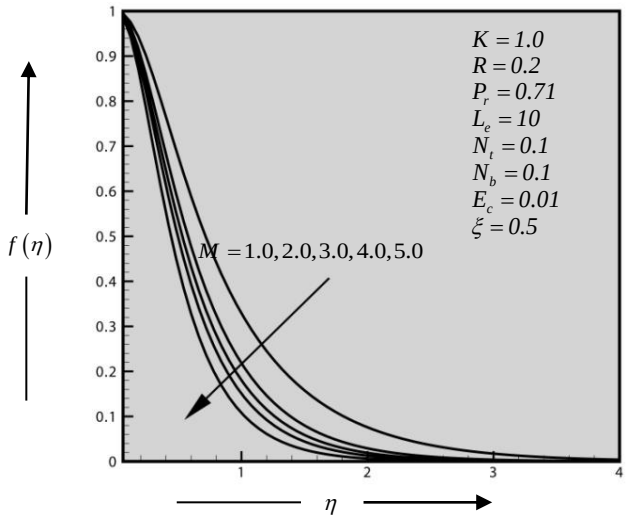

Figure 2. Primary velocity distribution for different values of Magnetic parameter (M).

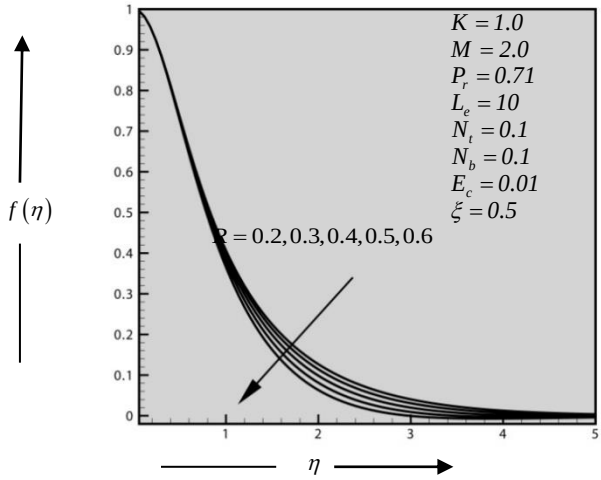

Figure 3. Primary velocity distribution for different values of Rotational parameter (R).

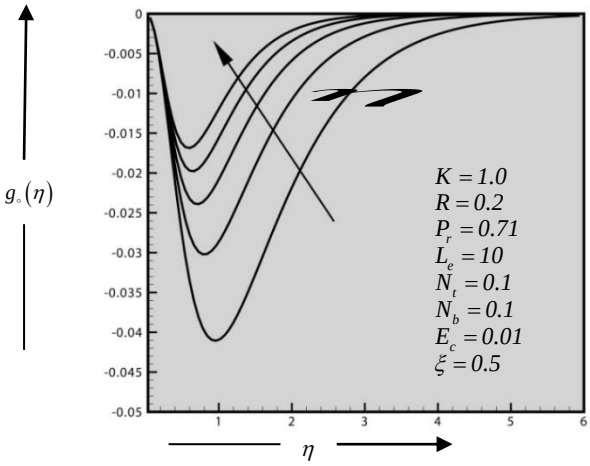

Figure 4. Secondary velocity distribution for different values of Magnetic parameter (M).

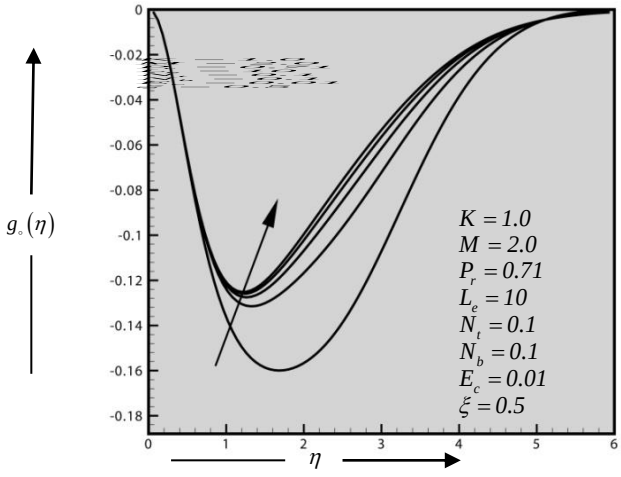

Figure 5. Secondary velocity distribution for different values of Rotational parameter (R).

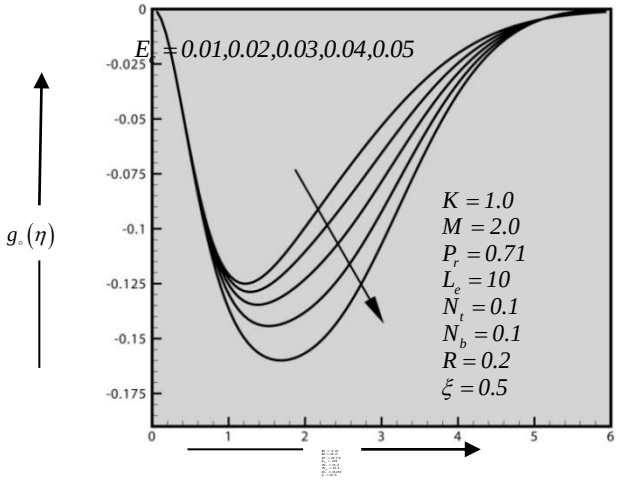

Figure 6. Secondary velocity distribution for different values of Eckert Number (E_c).

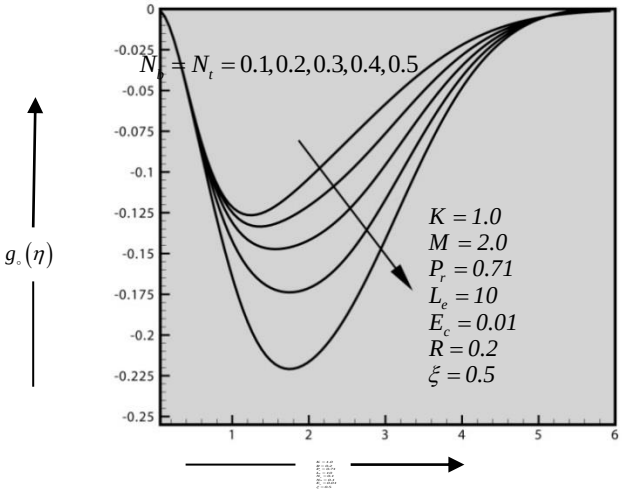

Figure 7. Secondary velocity distribution for different values of Brownian and Thermophoresis parameter $(N_b \& N_t)$.

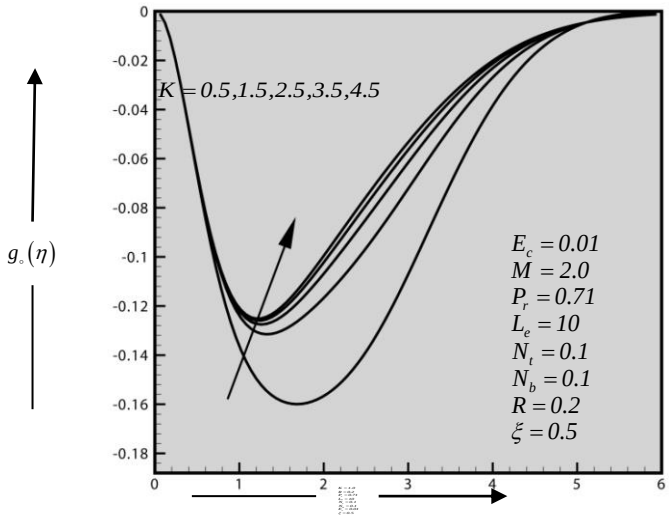

Figure 8. Secondary velocity distribution for different values of Radiation Parameter (K).

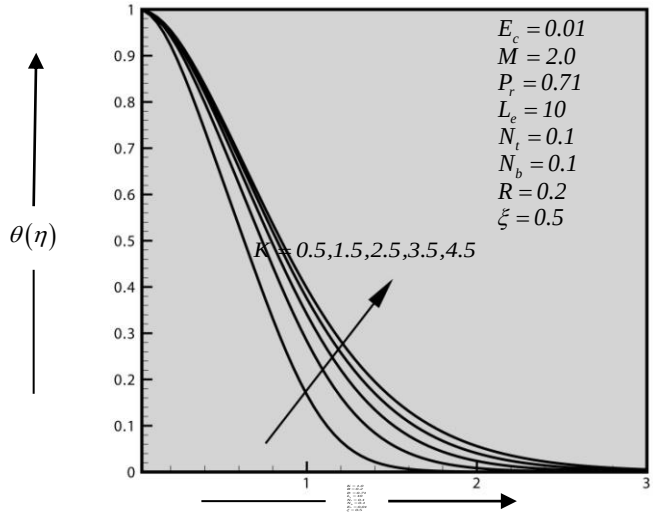

Figure 9. Temperature distribution for different values of Radiation Parameter (K).

The dimensionless temperature distribution $\theta(\eta)$ for different values of K is shown in Figure 9, which indicates that the $\theta(\eta)$ profiles increase as K increases. Similar trends are observed for P_r (Figure 10) and N_t (Figure 11). Figures 12, 13 and 14 illustrate the dimensionless concentration distribution $\varphi(\eta)$ for different values of K, N_t and L_e respectively. It is obvious that the $\varphi(\eta)$ profiles decrease with increase of K and L_e, while they increase with increase of N_t.

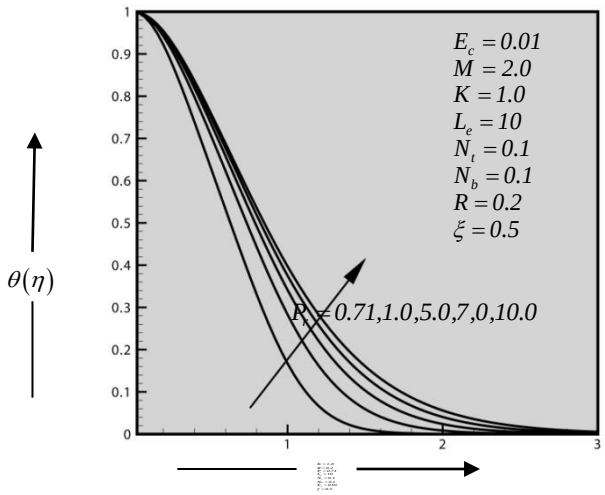

Figure 10. Temperature distribution for different values of Prandtl number (P_r).

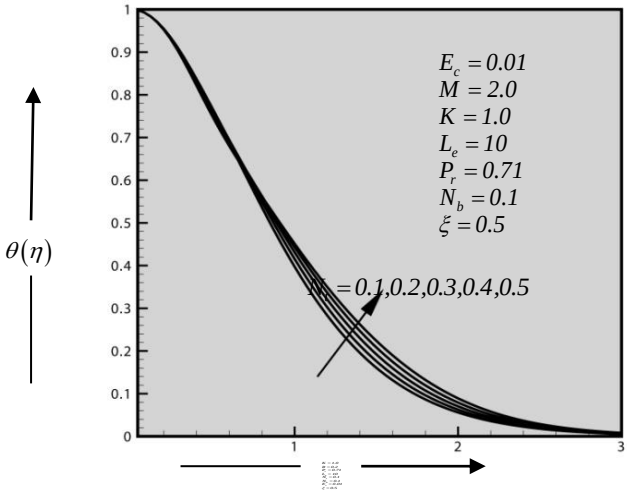

Figure 11. Temperature distribution for different values of Thermophoresis parameter (N_t).

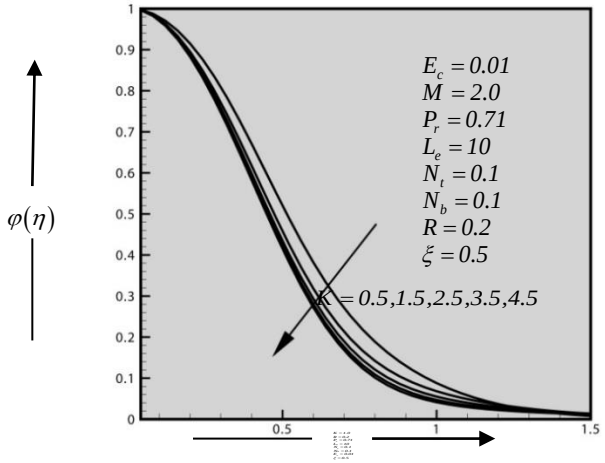

Figure 12. Concentration distribution for different values of Radiation Parameter (K).

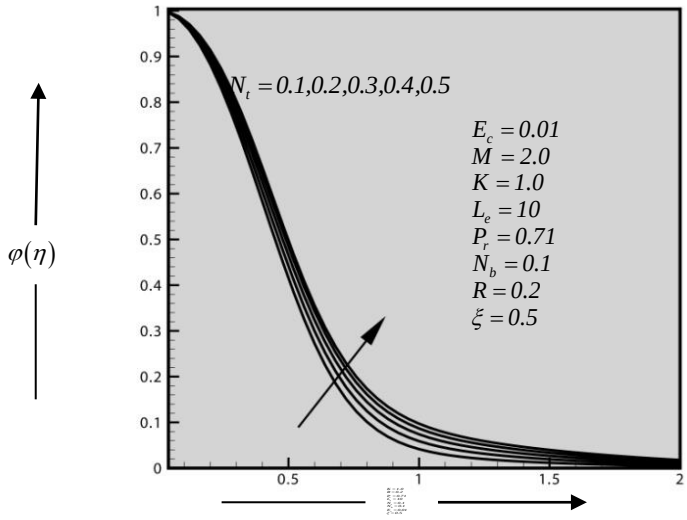

Figure 13. Concentration distribution for different values of Thermophoresis parameter (N_t).

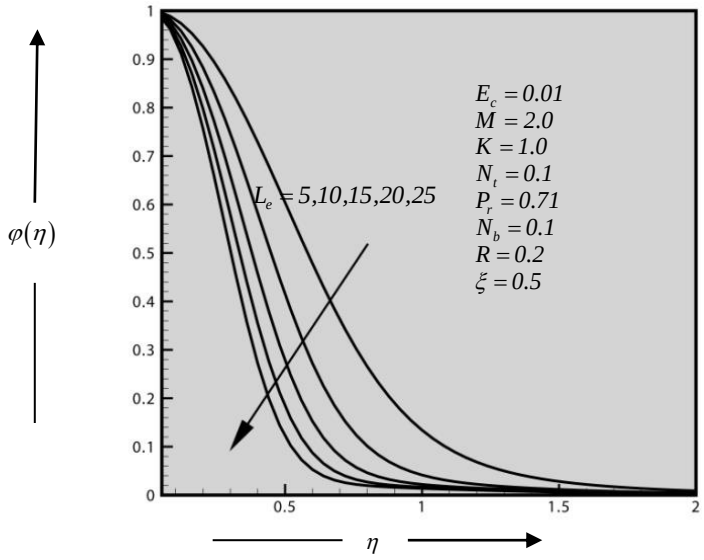

Figure 14. Concentration distribution for different values of Lewis number (L_e).

Table 1 and Table 2 summarize the effects of various parameters on skin friction, N_u and S_h. From Table 1, it can be observed that the skin friction components $(\tau_x \& \ \tau_z)$ increase as M and R increase, whereas N_u and S_h show very negligible change for $E_c = 0.01, K = 1.0, L_e = 10, P_r = 10.0, N_b = 0.1, N_t = 0.1$ and $\xi = 0.5$. Table 2 represents that as K and L_e increase, N_u decreases and S_h increases for $E_c = 0.01, R = 0.2, M = 2.0, P_r = 10, N_b = N_t = 0.1$ and $\xi = 0.5$. Also, the skin friction components show no effect on these parameters.

Table 1. Numerical values of τ_x, τ_z, N_u and S_h for $E_c = 0.01, K = 1.0, L_e = 10, P_r = 10.0, N_b = 0.1, N_t = 0.1,$ and $\xi = 0.5.$

R	M	τ_x	τ_z	N_u	S_h
0.2	1.0	0.0601304	0.0241291	0.2472051	0.0746482
0.3	2.0	0.1202315	0.0361870	0.2471988	0.0746532
0.4	3.0	0.1804018	0.0482738	0.2472078	0.0746428
0.5	4.0	0.2406415	0.0603895	0.2472154	0.0746342
0.6	5.0	0.3009504	0.0725342	0.2472214	0.0746274

Table 2. Numerical values of t_x, t_z, t_z and S_h for $E_c = 0.01, R = 0.2, M = 2.0,\ P_r = 10, N_b = N_t = 0.1$ and $\xi = 0.5.$

K	L_e	τ_x	τ_z	N_u	S_h
0.5	5.0	0.1202387	0.0241581	0.2732009	0.0440154
1.5	10.0	0.1202387	0.0241581	0.2305963	0.0933772
2.5	15.0	0.1202387	0.0241581	0.2112362	0.1145127
3.5	20.0	0.1202387	0.0241581	0.2004438	0.1259995
4.5	25.0	0.1202387	0.0241581	0.1936093	0.1331725

6. Conclusion

The thermal radiation effect on unsteady MHD heat and mass flow of a nanofluid past a stretching sheet in a rotating system is studied. The governing boundary layer equations are transferred to a system of non-linear ordinary coupled differential equations by similarity transformation. Numerical simulations are carried out for the mathematical model. The effects of various physical parameters such as Magnetic parameter, Rotational parameter, Radiation parameter, Prandtl number, Eckert number, Lewis number, Brownian motion parameter and Thermophoresis parameter on the heat and mass transfer characteristics are examined. The observed outcomes are briefly described below:

1. The primary velocity profiles decrease as the Rotational parameter increases, and vice versa in secondary velocity profiles.
2. As the Magnetic parameter increases, primary velocity profiles decrease whereas the secondary velocity profiles increase.
3. The secondary velocity and temperature profiles increase for increase in Radiation parameter whereas the concentration profiles show reverse patterns.
4. The secondary velocity profiles decreases as the Brownian and Thermophoresis parameters increase. Also temperature and concentration profiles increase as the Thermophoresis parameter increases.
5. The increase in Eckert number decreases the flow behaviour of secondary velocity profiles.
6. The temperature profiles increase as the Prandtl number increases, while the concentration profiles decrease as the Lewis number increases.

Acknowledgment

One of the authors, Md. Shakhaoath Khan, would like to acknowledge the National Science and Technology (NST) fellowship 2011 provided by the Ministry of Science and Technology, Government of People's Republic of Bangladesh for conducting this research as part of M.Sc. study.

References

Bachok N, Ishak A, Pop I. (2010). Boundary layer flow of nanofluid over moving surface in a flowing fluid, Int. J. of Thermal Sciences 49:1663–1668.

Beg OA, Khan MS, Karim I, Alam MM, Ferdows M. (2014). Explicit Numerical study of Unsteady Hydromagnetic Mixed Convective Nanofluid flow from an Exponential Stretching sheet in Porous media, Applied Nanoscience, 4(8): 943–957..

Brewster MQ. (1992). Thermal Radiative Transfer and Properties. John Wiley and Sons Inc., New York: USA.

Choi SUS. (1995). Enhancing Thermal Conductivity of Fluids With Nanoparticles, Development and Applications of Non-Newtonian Flows, DA Siginer and HP Wang, eds., ASME MD- vol. 231 and FED-vol. 66, USDOE, Washington, DC (United States), 99-105.

Ferdows M, Khan MS, Alam MM, Sun S. (2012). MHD Mixed convective boundary layer flow of a nanofluid through a porous medium due to an Exponentially Stretching sheet, Mathematical problems in Engineering, 3(7): 2551-155.

Ferdows M, Khan MS, Bég OA, Alam MM, (2014). Numerical Study of Transient Magnetohydrodynamic Radiative Free Convection Nanofluid Flow from a Stretching Permeable

Surface, Proceedings of the Institution of Mechanical Engineers, Part E: Journal of Process Mechanical Engineering, 228 (3):181-196.

Hossain MA, Takhar HS. (1996). Radiation effect on mixed convection along a vertical plate with uniform surface temperature, Int. J. Heat Mass Transfer 31: 243–248.

Khan WA, Pop I. (2010). Boundary layer flow of nanofluid past a stretching sheet, Int. J. Of Heat and Mass Transfer 53:2477-2483.

Khan WA, Pop I. (2011).Free Convection Boundary Layer Flow Past a Horizontal Flat Plate Embedded in a Porous Medium Filled with a Nanofluid, J. Heat Trans.133: 9.

Khan MS, Alam MM, Ferdows M. (2011). Finite Difference Solution of MHD Radiative Boundary Layer Flow of a Nanofluid past a Stretching Sheet, Proceeding of the International Conference of Mechanical Engineering; FL-011, BUET, Dhaka, Bangladesh.

Khan MS, Alam MM, Ferdows M. (2011). MHD Radiative Boundary Layer Flow of a Nanofluid past a Stretching Sheet, Proceeding of the International Conference of Mechanical Engineering and Renewable Energy. PI-105, CUET, Chittagong, Bangladesh.

Khan MS, Karim I, Ali LE, Islam A. (2012). MHD Free Convection Boundary layer Unsteady Flow of a Nanofluid along a stretching sheet with thermal Radiation and Viscous Dissipation Effects, International Nano Letters, 2 (24):1-9.

Khan MS, Alam MM, Ferdows M. (2013). Effects of Magnetic field on Radiative flow of a Nanofluid past a Stretching Sheet, Procedia Engineering, 56: 316-322.

Khan MS, Wahiduzzaman M, Karim I, Islam MS, Alam MM. (2014).Heat Generation Effects on Unsteady Mixed Convection Flow from a Vertical Porous Plate with Induced Magnetic Field, Procedia Engineering, 90: 238-244.

Kuznetsov AV, Nield DA. (2010). Natural convective boundary-layer flow of a nanofluid past a vertical plate, International Journal of Thermal Sciences 49: 243–247.

Nachtsheim PR, Swigert P. (1965). Satisfaction of the asymptotic boundary conditions in numerical solution of the system of non-linear equations of boundary layer type, NASA1965: TND-3004.

Nazmul I, Alam MM. (2008). Dufor and Soret Effects on Unsteady MHD Free Convection and Mass Transfer Fluid Flow Through a Porous Medium in a Rotating System, Bangladesh Journal of Sci. Res. 43: 159-172.

Raptis A, Singh AK. (1985). Rotation effects on MHD free convection flow past an accelerated vertical plate, Mechanical Resulation Communication 12: 31.

Sattar MA, Alam MM. (1994). Thermal diffusion as well as transpiration effects on MHD free convection and mass transfer flow past an accelerated vertical porous plate, Indian Journal of Pure and Applied Mathematics, 25:679.

Schichting H. (1968). Boundary Layer Theory, McGraw - Hill Book Co. NewYork, 1968.

Singh AK, Singh JN. (1989). Transient MHD free convection in a rotating system, Astrophysics and Space Science 162: 85.

Sakiadis BC. (1961). Boundary-layer behavior on a continuous solid surface: II-The boundary layer on a continuous flat surface, AIChE Journal 7: 221-225.

Takhar HS, Gorla RSR, Soundalgekar VM. (1996). Radiation effects on MHD free convection flow of a gas past a semi-infinite vertical plate, Int. J. Numer Meth Heat Fluid Flow 6:77-83.

Takabi B, Shokouhmand H. (2015). Effects of Al2O3-Cu/water hybrid nanofluid on heat transfer and flow characteristics in turbulent regime", International Journal of Modern Physics C; 26(4): 1550047.

Takabi B, Salehi S. (2014). Augmentation of the Heat Transfer Performance of a Sinusoidal Corrugated Enclosure by Employing Hybrid Nanofluid, Advances in Mechanical Engineering, 6:147059.

Wahiduzzaman M, Khan MS, Karim I, Biswas P, Uddin MS. (2015).Viscous Dissipation and Radiation effects on MHD Boundary Layer Flow of a Nanofluid past a Rotating Stretching Sheet, Applied Mathematics, 6: 547-567.

Wahiduzzaman M, Khan MS, Karim I. (2015).MHD convective stagnation flow of nanofluid over a shrinking surface with thermal radiation, heat generation and chemical reaction, Procedia Engineering, 105: 398-405.